JOURNAL OF AIRCRAFT
Vol. 31, No. 3, May–June 1994

Preliminary Piloted Simulation Studies of the HL-20 Lifting Body

Robert A. Rivers* and E. Bruce Jackson†
NASA Langley Research Center, Hampton, Virginia 23681
and
W. A. Ragsdale‡
Unisys Corporation, Hampton, Virginia 23665

NASA Langley Research Center is developing a lifting body vehicle, designated the HL-20, as one option of the proposed Personnel Launch System for NASA's future manned access to space requirements. Data derived from wind-tunnel and computational fluid dynamics analyses of the conceptual design led to the derivation of a flight simulator model to investigate the potential flight characteristics of the HL-20. A simulation investigation was initiated to determine if satisfactory unpowered horizontal landings could be accomplished. Control law design and trajectory development were directed toward this end. The study uncovered several deficiencies subsequently corrected through design changes, and it validated the predicted subsonic aerodynamic properties. Expanding the investigation to the Mach 4 to Mach 1 regime revealed flight characteristics necessitating the development of innovative control techniques. This article will present the significant results uncovered to date by flight simulator evaluations of a lifting body class of vehicle, and will demonstrate the effectiveness of flight simulation as an integrated part of the conceptual design phase.

Nomenclature

AR = aspect ratio
C_{l_β} = coefficient of rolling moment per degree angle of sideslip
C_{m_α} = coefficient of pitching moment per degree angle of attack
$C_{m_{\delta e}}$ = coefficient of pitching moment per degree of elevon deflection
C_{n_β} = coefficient of yawing moment per degree of sideslip
g = gravitation constant, 32.174 ft/s^2
h = height of c.g. of air vehicle, ft
L/D = lift-to-drag ratio
N_z = body axis normal acceleration, g
q_b = body axis pitch rate, deg/s
$\bar{q}$ = dynamic pressure, lb/ft^2
V_{rel} = Earth-relative velocity, ft/s
α = angle of attack, deg
β = angle of sideslip, deg
γ = flight path angle of c.g. of air vehicle, deg
δ_a = differential body flap position, deg
δ_c = pilot pitch stick command, in.
δ_e = elevon deflection, deg
δ_p = pilot rudder pedal command, in.
δ_w = pilot roll stick command, deg
θ = body pitch angle of air vehicle, deg
ϕ = body roll angle of air vehicle, deg

Received June 30, 1992; revision received March 3, 1993; accepted for publication April 23, 1993.

*Research Pilot/Aerospace Technologist, Aircraft Operations Branch. Senior Member AIAA.
†Aerospace Engineer, Aircraft Guidance and Controls Branch. Member AIAA.
‡Staff Engineer. Senior Member AIAA.

Introduction

THE HL-20 Lifting Body (Fig. 1) was proposed by the NASA Langley Research Center as a candidate for the Space Station Freedom Crew Emergency Rescue Vehicle (CERV) requirement. The HL-20 had evolved from studies of the Soviet Union's Bor lifting body flown from 1982 to 1986, and from NASAs prior lifting body research from 1965 to 1975.[1,2] The interest in utilizing this lifting body for CERV requirements resulted from the vehicle's impressive 1100-n.mi. cross-range capability (compared to the ~1000-n.mi. cross range of the Space Shuttle). CERV evolved into the Assured Crew Return Capability (ACRC) program, and the HL-20 became one of seven ACRC proposed designs.[3]

A NASA study to determine a suitable vehicle for the next manned Space Transportation System (STS) resulted in three candidate proposals, including a design developed as a complement to the current STS known as the Personnel Launch System (PLS). PLS is intended to provide access to space for people and small payloads using an expendable launch vehicle. The HL-20, refined during ACRC studies, was selected as one of two vehicle options for PLS.[4] HL-20 developmental

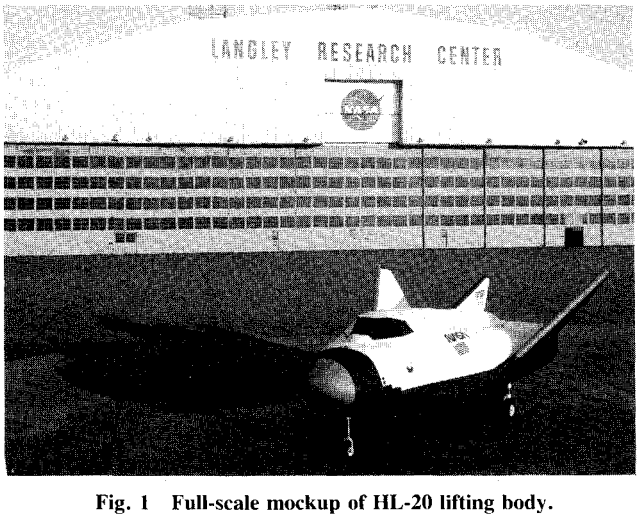

Fig. 1 Full-scale mockup of HL-20 lifting body.

research continued in wind-tunnel, computational fluid dynamics, human factors, and flight simulator studies. Reference 5 study set the current volume requirements limited by the ACRC specification to allow transport within the Space Shuttle cargo bay. A full-scale mock-up was built by North Carolina State and North Carolina A & T State Universities for NASA Langley for crew egress, cockpit visibility, and internal layout studies.

Well-documented previous lifting body experience had demonstrated a variety of stability and control problems for this class of vehicle.[1] Examples include postfabrication modifications necessary to alleviate Dutch roll problems with the M2-F2 and lateral control deficiencies with the HL-10.[6-9] Based on this experience, flight simulator investigations of the HL-20 conceptual design were initiated to evaluate the HL-20 predicted flight dynamics. This led to several design improvements and produced extensive data on the flight characteristics of the HL-20 from Mach 4 to touchdown. The initial goal of the study was to demonstrate that the HL-20 had the capability to perform satisfactory unpowered horizontal landings. This necessitated developing control surface mixing logic and simple feedback control laws that provided sufficient augmentation to accomplish this goal. These developments are presented first in this article, followed by a description of the vehicle dynamics, and finally, the specific results revealed during the simulator study.

Vehicle Description

The external physical characteristics of the HL-20 are presented in Fig. 2. The HL-20 conceptual design has emphasized efficient internal volume utilization. The internal layout contains a two-crew cockpit with seats mounted rather close to the forward windscreens to maximize the crew's field-of-view while minimizing windscreen size. Behind the cockpit are four rows of two seats for the planned eight-passenger manifest. Initial field-of-view studies have indicated an over-the-nose look-down angle from −14 deg directly forward to −22 deg at an off centerline angle of 40 deg. The HL-20 in its current configuration lands at a target pitch angle of +15 deg with tail scrape occurring between +18 and +20 deg. During the final flare, pitch angle increases at an almost linear rate of 1 deg for each 7 kt equivalent airspeed (KEAS) decrease. Landing at higher pitch attitudes is a concern due to both the reduction in over-the-nose visibility and the possibility of tail scrape.

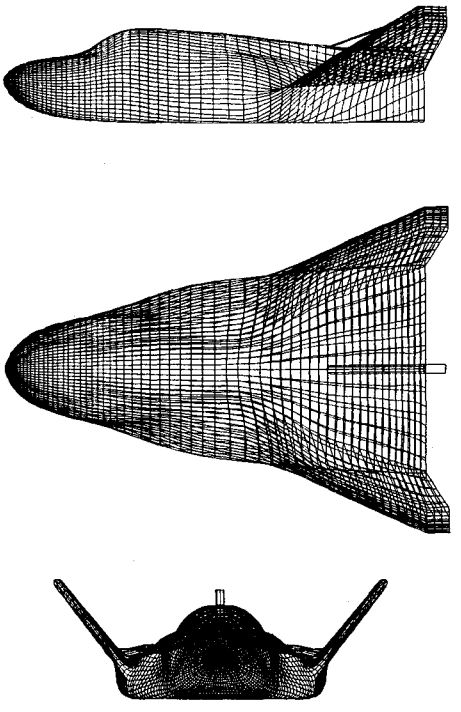

Fins:		Vehicle:	
Dihedral, ϕ_W, degrees	50	Weight, W_s, pounds	19,100
Sweep, Λ_W, degrees	62	Area, S_{ref}, ft^2	286.47
Incidence, α_{i_W}, degrees	1.25	Length, c_{ref}, ft	28.24
		Span, b_{ref}, ft	13.90
		Height of tail, h_t, ft	8.17
		Width, b_{max}, ft	22.43
		Center of Gravity, $x_{cg_{land}}$, ft	15.67

Fig. 2 HL-20 physical characteristics.

Simulator/Cockpit Description

The HL-20 real time simulation studies have been accomplished in NASA Langley's Visual Motion Simulator (VMS), a six-degree-of-freedom motion-base research simulator. Table 1 provides relevant information for the motion base. The visual scene delays have improved during the course of the study from approximately 140 ms to the current value of 115 ms. Cockpit instruments include an electronic attitude director indicator, electronic horizontal situation indicator, and a head-up display. A useful feature available on one of the instrument panel electronic displays is the surface position indicator which provides real-time indications of the positions of all seven control surfaces and a display of the control stick position for research analysis. The research pilot position contains a left-hand McFadden side stick controller. The mechanical characteristics of the side stick are included in Table 2.

Flight Controls Description

The current HL-20 design includes seven aerodynamic control surfaces. These include a relatively small (to mitigate reentry heating effects), all-movable vertical tail, two fin flaps or elevons, and four body flaps (two upper and two lower). This arrangement is similar to the earlier NASA lifting bodies. Pitch, roll, yaw, and speed brake inputs are separated by a control mixer into seven different control surface commands[10]

Table 1 Motion system performance

Degree of freedom	Position		Velocity	Acceleration
Horizontal, X	Forward	1.245 m	±0.61 m/s	±0.6 g
	Aft	1.219 m		
Lateral, Y	Left	1.219 m	±0.61 m/s	±0.6 g
	Right	1.219 m		
Vertical, Z	Up	0.991 m	±0.61 m/s	±0.6 g
	Down	0.762 m		
Pitch, θ	+30 deg		±15 deg/s	±50 deg/s^2
	−20 deg			
Roll, ϕ	±22 deg		±15 deg/s	±50 deg/s^2
Yaw, ψ	±32 deg		±15 deg/s	±50 deg/s^2

Table 2 Control stick mechanical characteristics

Left side stick; length (pivot point to top of grip), 7.5 in.				
Parameter	Pitch axis		Roll axis	
Maximum deflection, deg[a]	Forward	18	Left	20
	Aft	20	Right	20
Breakout force, lb	±1		±1	
Gradient, lb/in.	3.3		1.6	
Maximum force, lb	Forward	12	Left	6.5
	Aft	13	Right	6.5
Velocity limit, in./s	35		35	
Natural frequency, rad/s, Hz	23	(3.66)	16	(2.55)
Damping ratio	0.85		1.4	
Command scale factor, deg/in.[b]	Forward	1.5	25	
	Aft	2.5		

[a]20-deg deflection corresponds to 2.67 in. at 7.5 in. above the pivot point.
[b]Command scale factor is the ratio of effective elevator or aileron command to stick displacement. This does not correlate to control surface deflection or rotational rate commands.

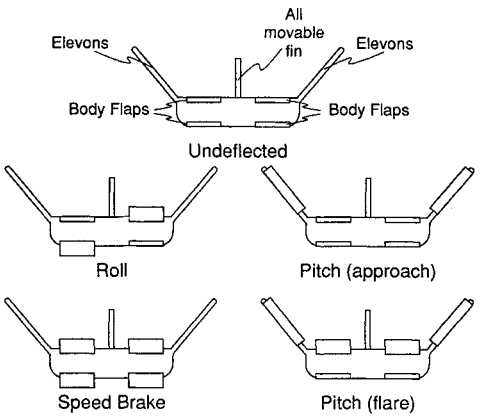

Fig. 3 Subsonic flight control mixing logic.

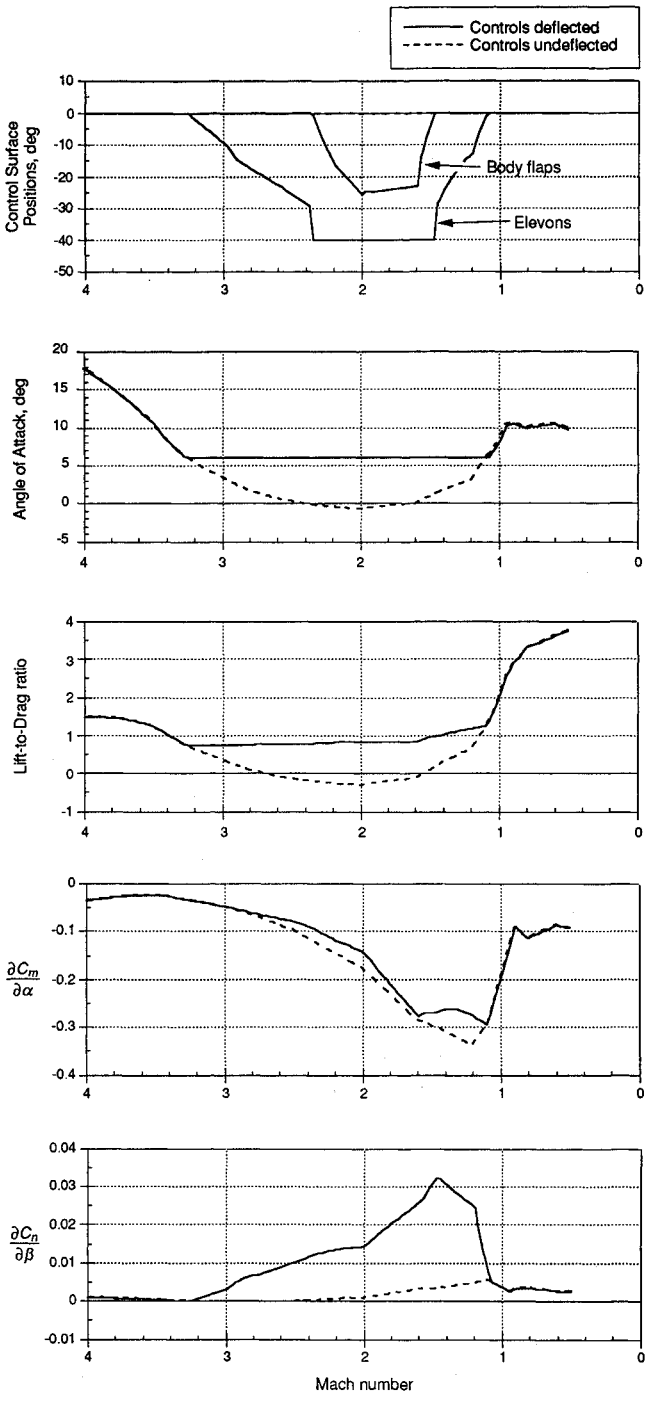

Fig. 4 HL-20 trimmed characteristics.

(Fig. 3). Pitch and roll are controlled through the side stick, and yaw through conventional rudder pedals. Speed brakes are commanded through a generic transport-type, pedestal-mounted lever. Longitudinal, lateral, and directional trim are available in all the control systems. Mach effects above Mach 1 cause sharp variances in trimmed L/D, C_{n_β}, and trimmed angle of attack (Fig. 4) and have necessitated a modification to the subsonic mixer logic. Supersonic flight characteristics are discussed in the results section.

It was realized at the outset that due to the high degree of adverse yaw coupled with the strong dihedral effects, the elevons would be unusable for lateral control. The elevons are actuated symmetrically for pitch control, and at higher angles of attack, are augmented by the upper body flaps. The body flaps are deployed simultaneously for speed brake and asymmetrically for roll control with roll control having priority over speed brake commands. The speed brake function is designed to provide longitudinally oriented aerodynamic reaction forces without pitch coupling. The upper and lower body flaps and a small amount of elevon are deployed in a nonlinear fashion in response to speed brake commands. Elevon deflection provides pitch trim compensation in the various flight control laws either explicitly or through a washout filter. The vertical tail is used for yaw control, and a yaw rate washout filter is employed to dampen short period yaw perturbations while not inhibiting steady-state yaw rate commands.[10]

Development of the Flight Control Systems

The unique aspects of a lifting body landing dictated care in designing the flight control system. The sink rate on outer glide slope can exceed 150 ft/s at an approach speed of 300 KEAS, and this must be reduced to less than 5 ft/s at 200 KEAS for touchdown. Using the level flight force balance equation

$$\dot{V} = -g/(L/D)$$

the deceleration rate on the inner glide slope is found to be approximately -5 kt/s using an L/D of 4.0 to account for the increased drag of the landing gear. This rapid decrease in dynamic pressure requires a continuously increasing, nonlinear angle of attack rate to maintain the requisite lift during a high work load phase of flight. In addition, the lift curve slope is comparatively shallow for wings of low aspect ratio (AR = 0.67 for the HL-20), necessitating a further increase in angle of attack. While conventional aircraft exhibit this characteristic, it is far more exaggerated in lifting bodies due to the rapid deceleration in the landing flare. The nonlinear increase in pitch attitude and angle of attack in the landing flare limit the potential of an alpha command flight control system (FCS) in the HL-20 simulation. Without any rate damping in the pitch axis, i.e., a pure angle of attack FCS, the HL-20 was found to be virtually uncontrollable due to a lightly damped short period mode.

A baseline control law was developed using the aerodynamic data from the first Aero Model, Version 1.0. This implementation utilized linearized flight control effects and did not contain any Mach effects. The control law consisted of a simple rate feedback system which provided increased damping in all three axes and an aileron-rudder interconnect (ARI) to improve turn coordination. The subsonic maximum L/D of 3.6 was found to be insufficient to attain level 1 (satisfactory) handling qualities for the landing task using the baseline control law.[11] Level 1 handling qualities are defined as aircraft handling qualities in which the pilot rating on the Cooper-Harper scale is 3 or better. Reference 12 provides a detailed description of the Cooper-Harper pilot rating scale. Further evaluation of control law development with Aero Model Version 1.0 (3.6L/D max) was not pursued since it was apparent that the maximum L/D of the vehicle was increasing with continued aerodynamic improvements. As a

result, the effects of augmented control laws and improved cockpit displays on unpowered handling qualities for a lower L/D vehicle were not obtained.

By changing the outboard fins from a flat-plate airfoil shape to a cambered airfoil with a flat undersurface, the maximum L/D was increased to 4.3.[13] This improvement resulted in the introduction of Aero Model Version 1.1, and level 1 handling qualities for the approach and landing task were demonstrated with this model using the baseline control law. Level 1 handling qualities for a similar vehicle were documented in-flight for the approach and landing task during the X-24B Lifting Body flight test program. The subsonic maximum L/D of the X-24B was 4.2, and the flight control system of the X-24B was similar to that of the HL-20 baseline control law in that each axis contained a rate damper for stability augmentation.[14]

Aero Model Version 2.0 was developed with full nonlinear data from Mach 4 to touchdown. Initial development of the advanced control laws was accomplished when Version 1.1 of the aero model was implemented. All of the control laws developed to date are available in both Version 1.1 and Version 2.0 of the aero model. Table 3 shows the interrelationships between the aero models, control laws, and evaluated tasks for the HL-20 design.

The baseline control law was not satisfactory in the pitch axis for the landing task since an exponentially increasing aft stick motion was required during the landing flare, and precise, repeatable landings were not easy to accomplish. Adding an autotrim feature improved the baseline system. The lateral-directional control laws were satisfactory and remained unchanged, i.e., in all of the control laws, only the pitch axis is augmented beyond simple rate feedback.[15] In the new system, known as Rate Command Attitude Hold (RCAH), the existing elevator position is fed back through a first-order filter and added to the existing elevator command, effectively placing a free integrator in the control loop which zeros any error between the commanded and actual vehicle rates. This same technique is used in the Shuttle flight control logic[16] and produces a control law that will pitch at a rate proportional to stick deflection and hold a nearly constant pitch attitude when the stick is released. Since angle of attack via pitch attitude must be increased nonlinearly (more rapidly as the speed decreases) in the landing flare, the RCAH system showed deficiencies in this flight phase due to its tendency for pilot induced oscillations (PIO). Rate command and RCAH systems have proven less than optimum in other applications for a variety of reasons. References 17–19 provide some background of the problems of an RCAH-type system for the landing flare maneuver. Additional comparative information is contained in Refs. 16, 20, and 21 which describes the Shuttle rate-command flight control system in the approach and landing phases of flight.

Flight path angle, or γ, is the parameter the pilot is ultimately interested in controlling during a landing. Since many pilots expect a pitch rate response from their inputs, it was believed that attempting to command flight path angle directly might result in PIO tendencies in the HL-20. By feeding back the rate of change of γ, however, it was believed that PIO may be kept to a minimum. This method became the basis for the Gamma Washout FCS and resulted in improved handling qualities in the landing phase. The limitation of the Gamma Washout System was in determining high-quality measurements of γ in flight. A better method was developed which estimated γ rate (deg/s) from the following equation with the vertical acceleration, or N_z, in g and V_{rel}, in ft/s as the variables:

$$\dot{\gamma} = \frac{57.3g(N_z - 1)}{V_{rel}}$$

N_z and V_{rel} can be derived accurately from a number of sources. The combination of γ rate (derived from N_z and V_{rel}) and pitch rate feedback combined with the pilot's stick inputs defined the NZQ control law. This control law will pitch at a rate proportional to the pilot's stick deflections and maintain 1g when the stick is released. The NZQ FCS performance is equivalent to that of the Gamma Washout system and has become the preferred control system for the HL-20 simulation due to its low susceptibility to PIO and its overall superior handling qualities.

In all of the four flight control systems, the pilot's pitch input is passed through a shaping function which can be varied from straight linear to pure quadratic. A value of 0.6 was experimentally determined to have the best characteristics where 0 yielded a linear law and 1 yielded a quadratic law. This allowed a lesser sensitivity for small stick inputs effectively increasing the dead band. The shaped command is passed through a gain to produce a pitch rate command, and in the Baseline and RCAH systems, no further active commands are utilized. In both the Gamma Washout and NZQ systems,

Table 3 Aero model, control law, and task matrix

Aero Model Version	Model features	Control laws	Tasks performed
1.0	3.2L/D max Subsonic only Linear control effects Fixed-base simulator No HUD	Baseline	HQRs for approach and landing task Evaluate and record HQRs with varied L/D, weight configurations Evaluate varied approach procedures
1.1	4.3L/D max Subsonic only Linear control effects Fixed and motion simulators HUD	Baseline RCAH Gamma washout NZQ	Develop and evaluate flight control system Refine approach procedures Evaluate crosswind landing capabilities Investigate c.g. envelope Determine off-nominal energy capabilities Develop HUD symbology Solve nose derotation problem HQRs for various control laws
2.0	4.3L/D max Mach 4.0 to touchdown Nonlinear control effects 6-degree-of-freedom motion base simulator HUD	Baseline HZQ	Investigate Mach 4.0 to 1.0 flight characteristics Modify flight control laws to accommodate new aero model HQRs for Mach 4.0 to 1.0 flight regime

Table 4 Approach longitudinal dynamics

Flight condition: $V = 300$ KEAS, $\gamma = -17$ deg, $\alpha = 5.9$ deg	
Open loop response, deg/deg (full order)	$\frac{\theta}{\delta_e} = -6.45 \frac{(s + 1/1.67)(s + 1/23.9)}{[s^2 + 2(0.17)(2.79)s + (2.79)^2][s^2 + 2(0.39)(0.076)s + (0.076)^2]}$
Closed loop response, deg/in. (short period equiv.)	$\frac{\theta}{\delta_c} \cong 14.13 \frac{(s + 1/1.38)}{(s + 1/0.15)(s + 1/0.4)} e^{-0.064s}$
Path/attitude dynamics, ft/deg	$\frac{h}{\theta} \cong \frac{1}{57.3} \frac{590}{s(1.67s + 1)}$

Table 5 Landing longitudinal dynamics

Landing condition: $V = 200$ KEAS, $\gamma = -1$ deg, $\alpha = 14$ deg	
Open loop response, deg/deg (full order)	$\frac{\theta}{\delta_e} = -3.55 \frac{(s + 1/2.65)(s + 1/23.6)}{[s^2 + 2(0.18)(1.85)s + (1.85)^2][s^2 + 2(0.26)(0.14)s + (0.14)^2]}$
Closed loop response, deg/in. (short period equiv.)	$\frac{\theta}{\delta_c} \cong 6.15 \frac{(s + 1/3.05)}{(s + 1/0.107)(s + 1/0.99)} e^{-0.037s}$
Path/attitude dynamics, ft/deg	$\frac{h}{\theta} \cong \frac{1}{57.3} \frac{338}{s(2.60s + 1)}$

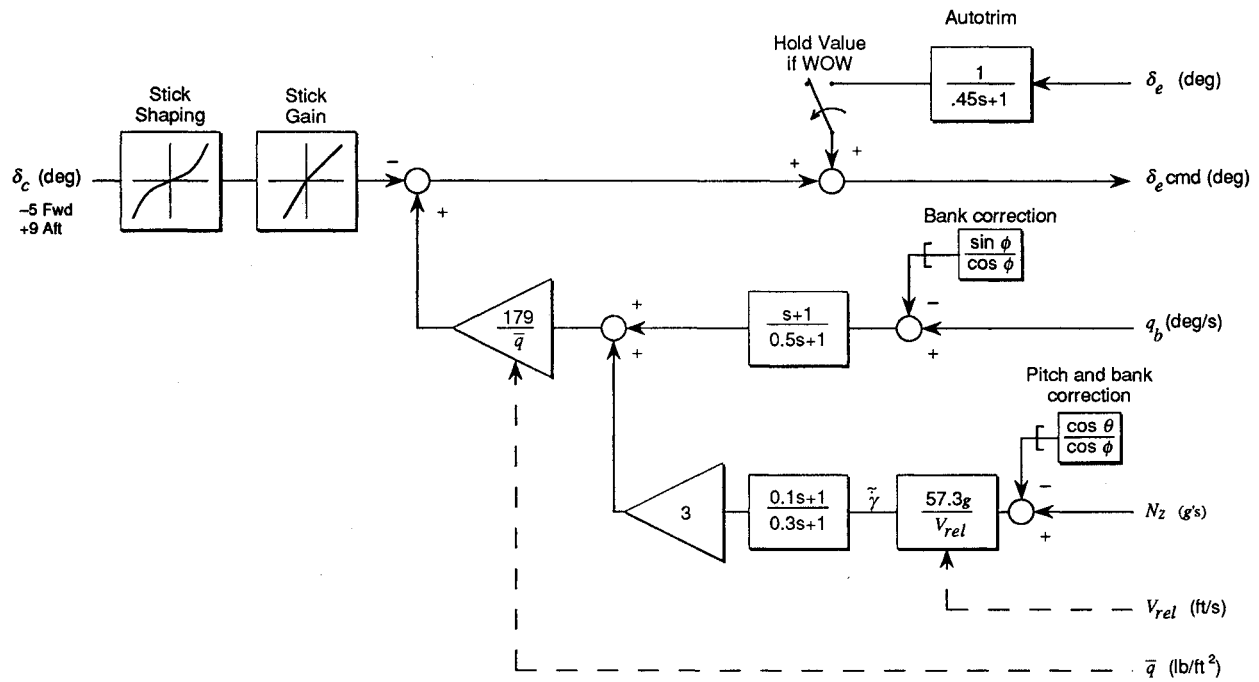

Fig. 5 NZQ pitch control law.

gamma rate is estimated and added to the pitch rate signal. In both cases, a fixed gain is employed to control the amount of pitch rate required to maintain gamma rate approximately zero with no pitch inputs. The command signal is then multiplied by a variable gain inversely proportional to dynamic pressure to compensate for variations in control effectiveness. The pitch trim command is determined by a lagged feedback of the present elevon deflection added to a speed brake compensator driving elevon trim whenever the speed brake is in motion. The elevon feedback is held at the value existing at weight on wheels (WOW) after touchdown. The current NZQ pitch control algorithm is shown in Fig. 5; a complete control law description is found in Refs. 10 and 15.

The total elevator command is the sum of the command input and the trim command. The elevator command is routed to simulated first-order elevon actuators with a 0.1-s time constant and a 40 deg up or down deflection limit, rate limited to 20 deg/s in the Aero Model Version 2.0. The artificial rate limit of 20 deg/s was experimentally determined in the simulator to be sufficient for required maneuverability, and is easily attainable within foreseeable hinge moment and actuator limits which have yet to be established for the HL-20.

Vehicle Dynamics

As shown in Tables 4 and 5, the open-loop longitudinal response of the HL-20 subsonically is very lightly damped in both short period and phugoid modes with a flight path lag time constant T_{θ_2} of 1.67 s in the approach condition and 2.6 s in the landing condition. Adding the NZQ flight control system to the open-loop aircraft gives the HL-20 a highly augmented set of longitudinal dynamics, characterized by two stable aperiodic roots in both flight conditions. This decoupled short period behavior has been exhibited by other successful aircraft, notably the Douglas DC-3.[22] In addition, the numerator zero in the pitch attitude to control stick response is

Table 6 Approach lateral-directional dynamics

Flight condition: $V = 300$ KEAS, $\gamma = -17$ deg, $\alpha = 5.9$ deg	
Open loop roll response, deg/s/deg (full order)	$\frac{p}{\delta_a} = 7.05 \frac{(s + 1/91)[s^2 + 2(0.15)(1.36)s + (1.36)^2]}{[s^2 + 2(0.21)(3.21)s + (3.21)^2][s^2 + 2(0.25)(0.28)s + (0.28)^2]}$
Open loop sideslip response, deg/deg (full order)	$\frac{\beta}{\delta_a} = 0.0034 \frac{(s - 1/0.0035)[s^2 + 2(0)(0.32)s + (0.32)^2]}{[s^2 + 2(0.21)(3.21)s + (3.21)^2][s^2 + 2(0.25)(0.28)s + (0.28)^2]}$
Equivalent closed loop roll response, deg/s/deg	$\frac{p}{\delta_w} = 4.55 \frac{(s + 1/1.38)}{(s + 1/0.103)(s + 1/0.627)}$
Equivalent closed loop sideslip response, deg/deg	$\frac{\beta}{\delta_w} = \frac{0.057}{(s + 1/0.71)} e^{-0.08s}$

Table 7 Landing lateral-directional dynamics

Flight condition: $V = 200$ KEAS, $\gamma = -1$ deg, $\alpha = 14$ deg	
Open loop roll response, deg/s/deg (full order)	$\frac{p}{\delta_a} = 2.8 \frac{(s - 1/50)[s^2 + 2(0.14)(1.9)s + (1.9)^2]}{[s^2 + 2(0.12)(3.61)s + (3.61)^2][s^2 + 2(0.94)(0.23)s + (0.23)^2]}$
Open loop sideslip response, deg/deg (full order)	$\frac{\beta}{\delta_a} = 0.68 \frac{[s^2 + 2(0.61)(0.35)s + (0.35)^2]}{[s^2 + 2(0.12)(3.61)s + (3.61)^2][s^2 + 2(0.94)(0.23)s + (0.23)^2]}$
Equivalent closed loop roll response, deg/s/deg	$\frac{p}{\delta_w} = \frac{23.7}{[s^2 + 2(0.48)(9.9)s + (0.9)^2]}$
Equivalent closed loop sideslip response, deg/deg	$\frac{\beta}{\delta_w} = \frac{0.32}{[s^2 + 2(0.36)(3.6)s + (3.6)^2]}$

no longer coincident with the flight path lag time constant, a trait exhibited by highly augmented aircraft.

The location of the subsonic instantaneous center of rotation of the vehicle in the longitudinal axis varies between 1.2–1.6 ft behind the pilot seat position, depending on flight condition. This results in conventional pitch acceleration cuing during longitudinal maneuvers.

The lateral-directional axis for the open-loop HL-20 exhibits lightly damped oscillatory behavior, as shown in Tables 6 and 7. The traditional roll and spiral modes are coupled to form a roll-spiral mode, or lateral phugoid. By feeding back body roll and yaw rates to the roll and yaw channels of the flight control system, however, the lateral dynamics become well damped.

Results of the Simulation Studies

When the HL-20 simulation study began, Aero Model Version 1.0 was evaluated, and the handling qualities of four different vehicle L/D configurations were investigated. The results of this study indicated that level 1 flying qualities were achievable in a vehicle of this type with a subsonic L/D ratio of 3.8 or higher.[11] The need to improve the L/D ratio of the Version 1.0 design had become apparent early in the study, and a subsonic L/D ratio of 4.3 was achieved[13] with the design changes resulting in Aero Model Version 1.1. The results of the simulation study since the implementation of Version 1.1 will be discussed below.

Approach and Landing Characteristics

The motivation for the increased L/D requirement was the high-energy bleed rate on the inner glide slope and in the final flare. The amount of "float time" in the final flare determines the amount of time the pilot has to perform the landing task and is directly related to the energy bleed rate. Prior to implementing Version 1.1, studies had shown that pilot handling quality ratings (HQRs) improved with lighter landing weights at a constant 3.2L/D ratio. This was due in part to slower touchdown speeds and more time available in the final flare resulting in a larger "landing window." With the implementation of the 4.3L/D ratio model, the landing window was large enough to merit a Level 1 flying qualities assessment from all evaluation pilots for the landing task using the baseline control law. The performance criteria for a desirable landing were 1) vertical velocity $\dot{h}$ less than -5 ft/s, 2) touchdown speed of 200 ± 10 KEAS, and 3) lateral position error of less than 15 ft. The average handling quality rating (Cooper-Harper) for all pilots surveyed (five research pilots and astronauts) for the landing task with the Version 1.1 aero model was 2.3, using the NZQ or Gamma Washout FCS. Since selecting an optimal flight control system for the HL-20 design was beyond the scope of the investigation, a rigorous piloted evaluation program was not undertaken.

Concurrent with the implementation of the 4.3L/D aero model (Version 1.1) was the development of three additional flight control systems, the RCAH, Gamma Washout, and NZQ control laws previously described, and the determination of the approach profile. The approach profile was defined by the vehicle L/D ratio and consisted of a -17-deg gamma outer glide slope (OGS) flown at 300 KEAS, a parabolic, 1.5 g preflare maneuver commenced at 1400-ft above ground level (AGL), and initially, a 1.5-deg inner glide slope (IGS), during which the landing gear deployment occurs at approximately 200-ft AGL in order to touchdown at 200 KEAS.

Optimizing the vehicle controllability in the final flare became the uppermost goal of the simulator evaluations. The vehicle was easily controllable during the subsonic approach profile with the most demanding phases being the preflare maneuver and the final flare. Reducing the nominal g required for the preflare maneuver to 1.25 diminished the preflare effort. Nonlinear shaping of the pitch input diminished the longitudinal sensitivity in the final flare. Flattening the IGS to -1 deg further improved touchdown performance by reducing the required final flare inputs. Investigating the touchdown position correlation with touchdown airspeed revealed that the HL-20 at a nominal approach weight of 19,100 lb will travel 71 ft in downrange distance for each knot deceleration in the final flare (compared to the Shuttle's 90 ft/kt during a typical approach).

The addition of motion cues to the simulation emphasized a derotation problem at touchdown. Due to a relatively aft

placement of the main landing gear, not enough nose-up pitching authority was available to prevent an excessive nose touchdown rate. The first attempted solution was to bias the upper body flaps to match the elevon position with WOW. Unfortunately, the resulting increase in pitching moment available led to an overly sensitive pitch response with a corresponding tendency to overrotate at touchdown. Moving the main landing gear forward 18 in. became the more viable solution, since this allowed enough elevon power to safely derotate. There was still a degree of longitudinal instability at touchdown, and repeatable derotation rates were not obtainable. The best derotation handling qualities occurred, however, in the baseline FCS with rate damping only. This indicated that the unacceptable derotation dynamics were caused by the autotrim feature in the FCS. The solution was to defeat the autotrim function with WOW (Fig. 5). Derotation must be completed by 170 KEAS, which is the lower limit of derotation control.

An extensive crosswind investigation demonstrated that the HL-20 configuration is very controllable in high crosswind landings. The design goal was 22-kt direct crosswind with projected main landing gear lateral velocity limits of 20 ft/s as the criteria. In order to minimize the main landing gear lateral velocity, slipped vs crabbed landing approaches were studied. This necessitated zeroing the ARI gain since the ARI would effectively oppose any attempts at cross-controlling. As a result, it was discovered that the ARI was not required in the subsonic regime because of the HL-20's inherent aerodynamic damping. Due to the very strong dihedral effect, with 50% rudder input, full opposite lateral inputs were insufficient to overcome the proverse roll. With crosswinds of 15 kt and above, it was not possible to align the vehicle nose with the runway with directional inputs without objectionable rolling effects. It was found that performing a slipped landing can reduce the crab angle up to 2 deg before reaching lateral control limits. The slip maneuver, unfortunately, also greatly increased the vehicle drag, reducing the L/D and increasing the energy bleed rate, and it was not easy to accomplish. Therefore, the crabbed landing crosswind technique is preferable.

Vehicle Characteristics with Varying Center of Gravity

The nominal c.g. for landing and abort weights is located at the 55.5% body length position, and the subsonic neutral point at these weights is located at 59% body length. The neutral point varies as a function of Mach number, reaching an aft limit of 67% body length from Mach 1.7 to Mach 1.3. The effects of c.g. variation were studied at weights ranging from 19,100 to 28,000 lb, with the c.g. varying from 48 to 62% body length. The HL-20 was found to be controllable with adequate longitudinal margins from 50 to 60% body lengths at all weights, although at the heavier weights longitudinal control saturation occurred in the final flare maneuver. A more extensive evaluation was accomplished at the approach weight, and it was noted that the aft limit was established at 62% body length due to the neutral directional stability point having been reached. Adverse yaw effects became apparent at 60% body length and were significant by 62% body length. Pitch stability was more than adequate with the NZQ control law, but earlier evaluations indicated that in the baseline control law the HL-20 would become longitudinally unstable with the c.g. aft of 60% body length. As the c.g. moved forward of 50% body length, the touchdown pitch attitude increased beyond 17 deg, which could result in a tail scrape at touchdown. This is due to the lifting body configuration. With the elevons and body flaps fully deflected upward, the coefficient of lift is lower at a given angle of attack, requiring a higher touchdown attitude to provide the same lift.

Vehicle Response to Off-Nominal Energy States

The HL-20's ability to recover from off-nominal energy situations has been impressive. At 15,000-ft AGL the HL-20 can perform a successful landing from as much as 4000-ft above glide slope and nominal approach speed. In the low-energy case at maximum L/D airspeed, the HL-20 can recover from as much as 3800-ft below glide slope. This is equivalent to correcting from essentially 25% above or below glide slope within 1 min and 5 miles of downrange travel. The low-energy technique is to capture the best L/D angle of attack (12.8 deg or about 230 KEAS at the approach weight of 19,100 lb) at approximately −13-deg gamma, and hold that attitude until slightly above glide path. The slight excess altitude can then be used in the ensuing pushover to regain the proper OGS airspeed of 300 KEAS. At least 250 KEAS will assure sufficient energy to execute the preflare maneuver. Correcting for a high-energy situation may require full manual speed brake deployment and a pushover to −35-deg gamma in the extreme. The current HL-20 speed brake model will allow the vehicle to achieve this gamma without appreciable increase in OGS optimum airspeed.

Vehicle Supersonic Characteristics

The introduction of Aero Model Version 2.0 data expanded the simulator flight envelope to Mach 4 and included nonlinear flight control effects. With slight modifications to the control laws, the HL-20 can be aerodynamically controlled at 90,000 ft without reaction control system jets which have yet to be modeled. A simple TACAN-based navigation algorithm is used to provide terminal area energy management (Fig. 6).

Several interesting aerodynamic characteristics have surfaced in the supersonic flight regime. Between Mach 2.5 and Mach 1.5 with undeflected control surfaces and c.g. at 55.5%, the HL-20 trims to −2-deg angle of attack. Full nose-up pitch controls are able to maintain the HL-20 at a maximum angle of attack of only +8 deg (Fig. 4). To alleviate pitch control saturation, the trajectory has been modified to fly at +6-deg angle of attack in this regime. This results in dynamic pressures building to an equivalent airspeed of approximately 400 kt. Further trajectory shaping above Mach 4 may reduce this problem. The NZQ pitch control law used for subsonic flight was found to be adequate for control and damping in the

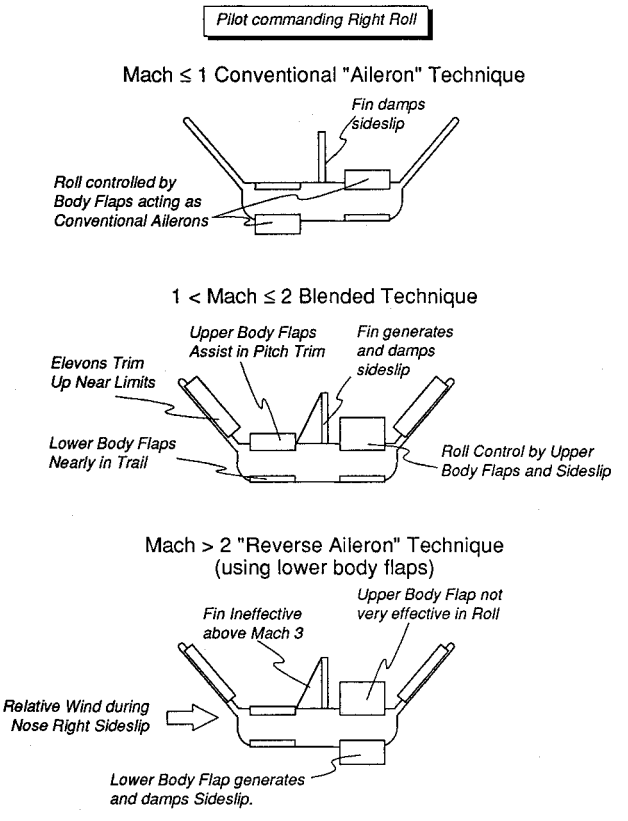

Fig. 6 Supersonic flight control mixing logic.

supersonic regime. This control law has been used from Mach 4 to touchdown by increasing the forward loop gain to compensate for the variation in $C_{m_{\delta_e}}$ vs Mach number. The feedback gains for the pilot's stick inputs, pitch rate, and vertical acceleration are the same.

Lateral control problems have been uncovered due to the lack of rudder effectiveness above Mach 3 and the adverse yaw produced by the lower body flaps when conventional lateral inputs are made. To correct this, the lower body flap deflections are deliberately reversed to take advantage of the adverse yaw. The high C_{l_β} of the vehicle results in a roll in the desired direction. Beginning at Mach 2, this reverse gain is ramped down and is absent by Mach 1. Sideslip angle and sideslip angle rate (derived from angle of attack, roll rate, and yaw rate) feedbacks are also added to the lower body flap deflection command, providing sideslip control and damping (Fig. 6). The resulting roll rates are limited to approximately 13 deg/s (compared to the 7 deg/s rate limit for the Shuttle) in supersonic flight. Upper body flaps are applied in the conventional manner at all Mach numbers. Rudder alone is very effective in rolling the vehicle below Mach 1.5. With the modifications described above, adequate supersonic control of the HL-20 is provided by the NZQ pitch and baseline lateral control laws.

Concluding Remarks

The HL-20 has been demonstrated to be a viable design for successfully accomplishing unpowered, horizontal landings. The flight simulation studies uncovered several deficiencies which have been corrected in the conceptual stage. These included the requirement for an increased subsonic L/D to achieve Level 1 handling qualities with only a rate-damped FCS, and the requirement to move the main landing gear forward to alleviate the nose derotation problem at touchdown. Much flight simulation effort was spent in investigating the open and closed loop vehicle dynamics, and in developing and finely tuning the various flight control systems. Flight path angle rate command control laws were found to be superior to pure pitch rate command control laws for the landing task. The approach profile was modified to account for vehicle dynamics on the inner glide slope and in the final flare. In studying several off-nominal conditions, it was discovered that the HL-20 design is quite robust and forgiving on approach and consistent on landing. Research is continuing in the area of supersonic flight dynamics. The decision to utilize flight simulation research this early in the design process to validate the concept has proven to be invaluable. As a result of the flight simulation study, the HL-20 design appears capable of accomplishing the difficult task of approach from Mach 4 to landing.

References

[1]Hallion, R. P., *On the Frontier, Flight Research at Dryden 1946–1981*, NASA SP-4303, 1984, pp. 147–172.

[2]Asker, J. R., "NASA Design for Manned Spacecraft Draws on Soviet Subscale Spaceplane," *Aviation Week and Space Technology*, Sept. 24, 1990, p. 28.

[3]Ware, G. M., Spencer, B., Jr., and Micol, J. R., "Aerodynamic Characteristics of Proposed Assured Crew Return Capability (ACRC) Configurations," AIAA Paper 89-2172, July 1989.

[4]Piland, W. M., Talay, T. A., and Stone, H. W., "Personnel Launch System Definition," International Astronautical Federation Paper 90-160, Oct. 1990.

[5]Ehrlich, C. F., Jr., and Stone, H. W., "Personnel Launch System/Advanced Manned Launch System (PLS/AMLS) Operational Support Analysis and Reliability/Maintainability Analysis," Rockwell International Space Systems Div., SSD90D0093/4, Downey, CA, Aug. 1990.

[6]Thompson, M. O., Peterson, B. A., and Gentry, J. R., "Lifting-Body Flight Test Program," *Proceedings of the Tenth Symposium of the Society of Experimental Test Pilots*, Society of Experimental Test Pilots, Lancaster, CA, 1966, pp. 99–120.

[7]Kempel, R. W., "Analysis of a Coupled Roll-Spiral-Mode, Pilot-Induced Oscillation Experienced with the M2-F2 Lifting Body," NASA TN D-6496, Sept. 1971.

[8]Painter, W. D., and Kock, B. M., "Operational Experiences and Characteristics of the M2-F2 Lifting Body Flight Control System," NASA TM X-1809, June 1969.

[9]Kempel, R. W., and Manke, J. A., "Flight Evaluations of HL-10 Lifting Body Handling Qualities at Mach Numbers from 0.30 to 1.86," NASA TN D-7537, Jan. 1974.

[10]Jackson, E. B., Cruz, C. I., and Ragsdale, W. A., "Real-Time Simulation Model of the HL-20 Lifting Body," NASA TM-107580, July 1992.

[11]Jackson, E. B., Rivers, R. A., and Bailey, M. L., "Effect of Lift-to-Drag Ratio Upon Pilot Rating for a Preliminary Version of the HL-20 Lifting Body," AIAA Paper 91-2890, Aug. 1991.

[12]Cooper, G. E., and Harper, R. P., Jr., "The Use of Pilot Rating in the Evaluation of Aircraft Handling Qualities," NASA TN D-5153, April 1969.

[13]Ware, G. W., Spencer, B., Jr., and Micol, J. R., "Aerodynamic Characteristics of the HL-20 and HL-20A Lifting-Body Configurations," AIAA Paper 91-3215, Sept. 1991.

[14]Manke, J. A., and Love, M. V., "X-24B Flight Test Program," *Proceedings of the Nineteenth Symposium of the Society of Experimental Test Pilots*, Society of Experimental Test Pilots, Lancaster, CA, 1975, pp. 129–154.

[15]Jackson, E. B., Ragsdale, W. A., and Powell, R. W., "Utilization of Simulation Tools in the HL-20 Conceptual Design Process," AIAA Paper 91-2955, Aug. 1991.

[16]Myers, T. T., Johnston, D. E., and McRuer, D., "Space Shuttle Flying Qualities and Flight Control System Assessment Study," NASA CR-170391, June 1982.

[17]Chalk, C. R., "Flying Qualities of Pitch Rate Command/Attitude Hold Control Systems for Landing," *Journal of Guidance, Control, and Dynamics*, Vol. 9, No. 5, 1986, pp. 541–545.

[18]McRuer, D., "A Perspective on Superaugmented Flight Control: Advantages and Problems," *Journal of Guidance, Control, and Dynamics*, Vol. 9, No. 5, 1986, pp. 530–540.

[19]Powers, B. G., "Space Shuttle Longitudinal Landing Flying Qualities," *Journal of Guidance, Control, and Dynamics*, Vol. 9, No. 5, 1986, pp. 566–572.

[20]Myers, T. T., Johnston, D. E., and McRuer, D., "Space Shuttle Flying Qualities and Flight Control System Assessment Study—Phase II," NASA CR-170406, Dec. 1983.

[21]Walker, H. J., "Analytic Study of Orbiter Landing Profiles," NASA TM-81363, Sept. 1981.

[22]McRuer, D., Ashkenas, I., and Graham, D., *Aircraft Dynamics and Automatic Control*, Princeton University Press, Princeton, NJ, 1973, p. 709.